Journal of Engineering Science and Technology
6th EURECA 2016 Special Issue May (2017) 58 - 70

CREATININE ADSORPTION BY ACTIVATED CARBON FIBRE (ACF) DERIVED FROM EMPTY FRUIT BUNCH (EFB) FIBRE

IVAN V. K. CHAI[1], X. Y. LIM[2], T. LEE[1,*]

[1]School of Engineering, Taylor's University, Taylor's Lakeside Campus,
No. 1 Jalan Taylor's, 47500, Subang Jaya, Selangor DE, Malaysia
[2]School of Engineering and Physical Sciences, Heriot-Watt University Dubai Campus,
Dubai International Academic City, P.O. Box 294345, Dubai, United Arab Emirates
*Corresponding Author: appleeting38@hotmail.com

Abstract

Adsorption is an important process in the haemodialysis treatment to treat patients with kidney failure. Adsorption membranes in haemodialysis systems are usually made of synthetic polymers but these membranes do not have high efficiency in removing uremic toxins such as urea, uric acid and creatinine. Thus, it is suggested to replace the current membranes with a new material that has high adsorption capability as well as being lightweight and low cost. This study suggests that activated carbon may be a potential replacement of current haemodialysis membranes. Activated carbon fibre is chosen due to their better adsorptive characteristics compared to granular and powder activated carbon. Empty fruit bunch fibre is chosen to produce activate carbon fibre because it is easily available in abundance throughout the year and has low commercial value. There is not much information available on creatinine adsorption using activated carbon fibre derived from empty fruit bunch fibre. Cleaned empty fruit bunch fibre is impregnated with 4 different chemicals to produce activated carbon fibre. The effects of these chemical treatments on the pore characteristics and physiochemical properties are studied. Activated carbon fibre samples are produced via pre-carbonisation chemical treatment followed up by carbonisation at 400 °C and activation at 900 °C. Samples exhibited Type I isotherm which indicates the presence of micro and mesoporous structure. The sample treated with phosphoric acid has the highest BET surface area of 1493 m^2/g and pore volume of 0.782 cm^3/g compared to other samples. Carbon burn-off of activated carbon fibre sample treated with phosphoric acid proved to be 86% which is the highest among all samples despite having the best adsorbing capability. This work has shown that activated carbon fibre treated with phosphoric acid has the potential in replacing the current membrane used in the current haemodialysis system with creatinine removal of 70% and urea removal of 68% which is higher than the conventional haemodialysis membrane.

Keywords: Creatinine, Adsorption, Activated carbon fibre, Empty fruit bunch fibre.

Nomenclatures

Q_o	Initial creatinine concentration, umol/g
Q_{eq}	Adsorbed creatinine concentration when equilibrium first Reached, umol/g
W	Final weight of raw EFB fibre, g
w_o	Initial weight of raw EFB fibre, g

Greek Symbols

θ	Carbon burn-off, wt%

Abbreviations

ACF	Activated Carbon Fibre
BET	Brunauer, Emmett and Teller
EFB	Empty Fruit Bunch
FTIR	Fourier Transform Infrared Spectroscopy
XRD	X-ray Diffraction

1. Introduction

Kidney failure is a syndrome where the kidneys could not fulfil their tasks in filtering blood. This kind of syndrome leads to an accumulation of molecules; called uremic toxins which are normally eliminated by healthy kidneys. People that have kidney failure is unable to separate these uremic toxins such as urea, uric acid and creatinine and has to be treated by the haemodialysis technique [1]. The haemodialysis process is where two liquids are separated by a semi-permeable membrane that enables an exchange of molecules small enough to diffuse through the pores. When blood is in contact with one of the sides of the semi-permeable membrane, substances such as body waste and inorganic salts pass through into a sterile solution called the dialysate. However, this method of treatment is not efficient as patients have to go through the treatment 3 to 4 times a week where each session lasts up to 4 hours [2].

Research and development towards the improvement of the haemodialysis system has been done throughout the years. The invention of hollow fibre dialysers have helped in increasing the efficiency in uremic toxin removal as well as new discovery of different materials to help in uremic toxin removal. However, the efficiency is not high and the haemodialysis machine is rather not portable. Artificial kidney is one of the methods suggested by Hakim and Lumley to increase the functionality of the body to remove uremic toxins [3]. The vision of this artificial kidney is to be able to remove uremic toxins efficiently, light weight and low cost. This may be solved if the membrane of the haemodialysis treatment in removing uremic toxins is upgraded to a more effective and low cost adsorbent [4].

Activated carbon may be the solution to this as the usage of activated carbon can be seen in wastewater treatment and air purification applications due to the high effectiveness in adsorption [5]. Activated carbon is defined as a solid and porous carbonaceous material with high porosity and large surface area [6]. Activated carbon can found in 3 forms; powdered, granular and fibre [7]. Among these 3 forms, activated carbon fibre (ACF) has the highest adsorbing capability.

There are many materials that can be made into activated carbon such as tea and coffee waste, peanut shells and wheat wastes which are of low cost materials [8].

This study has chosen empty fruit bunch (EFB) fibre to produce ACF as it is an agricultural waste generated from the oil palm industry, which is available in abundance throughout the year and has very low commercial value. It is naturally in a fibrous shape which makes it suitable to be made into ACF. ACF has a higher commercial value compared to other activated carbon types due to its higher adsorptive characteristics [9].

ACF or common activated carbons can be produced by involving a 2-step process; carbonisation and activation. Carbonisation can be done using combustion or pyrolysis [10]. The purpose of the carbonisation step is to remove any volatile compounds in the EFB fibre which will give rise to the number of pores in the fibre which is responsible for its adsorptive characteristics. Carbonisation is typically done at 400-600 °C. However, carbonisation done at an elevated temperature not only increases the carbon content but the ash content as well. This is due to greater decomposition of biomass at higher temperatures [11]. Comparison between combustion and pyrolysis was done and it showed that carbon content in biomass samples decreases at 400 °C and samples undergone pyrolysis has lower carbon burn-off (77.2 %) compared to samples undergone combustion (80.8 %) [9]. The activation step is to increase the pore diameter and volume to enhance the porosity of the activated carbon. It can be separated into chemical activation and physical activation. Chemical activation involves the impregnation of the precursor of the activated carbon with chemical activating agents. The commonly used activating agents are sodium hydroxide (NaOH), potassium hydroxide (KOH), sulphuric acid (H_2SO_4) and phosphoric acid (H_3PO_4) [11-15]. Physical activation is commonly done by heating the carbon at a range of 800 to 1000 °C [10]. Physical activation requires the carbon sample to be carbonised in an inert atmosphere and subsequent activation is done with oxidising gases such as carbon dioxide (CO_2), steam or air. In this work, carbonisation is done at 400 °C and activation at 900 °C as these conditions are the optimum conditions in synthesis of ACF according to the work of Ooi and co-workers [7].

This study work focuses on the comparison between different chemical-treated EFB fibres in their ability in adsorbing creatinine as a possible method to apply these material into the current haemodialysis treatment. The performance of the EFB fibre derived ACF in adsorbing creatinine is evaluated based on the composition and pore characteristics of each different chemical-treated EFB fibre derived ACF. The adsorbing performance of the ACF samples produced is also compared between creatinine adsorption and urea adsorption.

2. Methods

2.1. Materials

EFB fibre is collected from United Palm Oil Mill Sdn. Bhd. Nibong Tebal, Penang, Malaysia to be used as raw material. The EFB fibre is then cleaned with 5% nitric acid (HNO_3) and rinsed with distilled water until the pH reaches approximately 5. The cleaned EFB fibre is then dried in an oven overnight at 105 °C which is in accordance to the ASTM D2867-09 standard for moisture removal [16]. Sodium hydroxide (NaOH), potassium hydroxide (KOH), sulphuric acid (H_2SO_4) and phosphoric acid (H_3PO_4) are used as activating agents.

2.2. Sample preparation

Four sets of 12 g of cleaned EFB fibre is impregnated with concentrated NaOH, KOH, H_2SO_4 and H_3PO_4 (85 %) at an acid/alkali-to-fibre ratio of 3:4 (ml:g). An oxygen deficient atmosphere during pyrolysis is created by allowing a flow of nitrogen (N_2) gas at a flow rate of 100 ml per minute. The samples are then pyrolysed separately at 400 °C for 1 hour at a heating rate of 10 °C per minute. After pyrolysis, the samples are then left to cool to room temperature. The char after pyrolysis is then weighed prior to the activation step. The furnace temperature during the activation process is set at 900 °C at a heating rate of 10 °C per minute and the flow of N_2 gas is set at 100 ml per minute. At 900 °C, the flow of N_2 gas is stopped and changed to CO_2 gas at a flow rate of 100 ml per minute for 1 hour. After 1 hour, the flow of CO_2 gas is stopped and changed back to N_2 gas at a flow rate of 100 ml per minute. The sample is then cooled down to room temperature in the N_2 gas flow [9]. After activation, weight of each sample is measure and recorded again for the carbon burn-off analysis. Each sample is assign with sample codes as tabulated in Table 1.

Table 1. Samples identification.

Sample Code	Remarks
ACF_PA	EFB fibre derived ACF treated with H_3PO_4 (85%)
ACF_SA	EFB fibre derived ACF treated with H_2SO_4 (85%)
ACF_PH	EFB fibre derived ACF treated with KOH (85%)
ACF_SH	EFB fibre derived ACF treated with NaOH (85%)

2.3. Sample characterisation

By using the data of the weight measure before carbonisation, after carbonisation and after activation, the carbon burn-off, Θ (%) for the ACF can be calculated using the formula below:

$$\theta = \frac{w_0 - w}{w_0} \times 100\% \quad (1)$$

where, w_o is the initial weight of the raw EFB fibre (g) and w is the final weight of the ACF (g). Nitrogen adsorption isotherm at 77 K is done using Micromeritics Instrument system after a gas pre-treatment at 300 °C for 5 hours. Pore characteristics such as surface area, micropore volume and pore size distribution are determined from the nitrogen adsorption isotherms utilising Branauer-Emmett-Teller (BET) model. Nitrogen adsorption on the samples are carried out from relative pressure (P/P_o) of 0.01 to 0.99 [17]. The crystalline structure of the produced ACF is determined using the X-Ray Diffraction (XRD) analysis which included a scan range of 10° to 90° with a step size of 0.02° and step time of 0.05 seconds. The surface chemistry of the produced ACF samples is determined using the Fourier Transform Infrared Spectroscopy (FTIR) at a wavenumber ranging from 650 to 4000 cm^{-1} for 16 cycles.

2.4. Creatinine adsorption test

A creatinine solution with a concentration of 2 mg/dL is prepared to simulate the minimum concentration of creatinine concentration in the blood before undergoing

haemodialysis [18]. A standard calibration curve was developed by measuring the UV-Vis absorbance intensity of a series of creatinine solutions with known and varied concentrations using the UV-Vis spectrophotometer at a wavelength of 510 nm [19]. Creatinine adsorption is conducted for all ACF samples and the intensities of the creatinine samples at various time intervals are measured using the UV-Vis spectrophotometer. The intensities of the solution are then compared with the calibration curve to determine the adsorption amount by each ACF sample.

2.5. Urea adsorption test

A urea solution with a concentration of 120 mg/dL is prepared to simulate the average concentration of urea concentration in the blood of patients before undergoing haemodialysis [20]. A standard calibration curve was developed by measuring the UV-Vis absorbance intensity of a series of urea solutions with known concentration using the UV-Vis spectrophotometer at a wavelength of 200 nm [7]. Urea adsorption is conducted for all ACF samples and the intensities of the urea samples at various time intervals are measured using the UV-Vis spectrophotometer. The intensities of the solution are then compared with the calibration curve to determine the adsorption amount by each ACF sample.

3. Results and Discussion

3.1. Carbon burn-off

Carbon burn-off is a commonly used guideline to determine the yield of activated carbon. The higher the carbon burn-off, the lower the yield percentage [21]. Burn-off means the degree of carbon loss during the production of activated carbon. A higher carbon burn-off also means that there is a need to use more materials to produce the desired activated carbon which will lead to increase in cost for production. The carbon burn-off results shown in Table 2 proves the quality of the ACF produced in this work.

All samples were pre-treated with different chemicals (NaOH, KOH, H_2SO_4 and H_3PO_4). As an overall, the carbon burn-off for the sample ACF_PA is highest among all the samples produced. Addition of H_3PO_4 into the raw fibre samples may have facilitated in the conversion of aliphatic compounds, such as cellulose and hemicellulose to aromatic compounds [22]. The higher percentage in the overall carbon burn-off may also mean that more volatile compounds are removed due to the H_3PO_4 treatment. As compared to the ACF_SA sample, ACF_SA has a higher carbon burn-off at the post-carbonisation stage. This is due to the removal of water from cellulose and this would result in a higher weight loss, causing a higher carbon-burn off [23]. H_2SO_4 is distributed among the cellulose microfibrils then the H_2SO_4 would extract water from the cellulose and water would be removed from the surface of the fibres. The total carbon burn-off of the acid-treated ACF in this study falls in the region of 75-85% which is considered to be comparable to other works on oil palm empty fruit bunch which have a carbon burn-off percentage of approximately 72-96% [21-22].

The carbon burn-off analysis for both alkali treatments are not available due to the fact that the concentration of the alkali used is too high. Metal ion in alkali solutions are usually in the form of aquo ions. These aquo ions are most likely to

enter the crystallisation region of the cellulose of the fibre samples. A concentration of 15-20% would start to cause swelling at the crystalline region [24]. Thus, a concentration used at this work which is 80% would have already destroyed the crystalline structure of the fibre samples, causing the whole structure of the sample to disintegrate. This would explain the unavailable data for the carbon burn-off and further analysis done in this work.

Table 2. Carbon burn-off percentage of ACF samples.

Sample	Initial Weight (g)	Post-Carbonisation Weight (g)	Post- CO_2 Activation Weight (g)	Total Carbon Burn-Off (%)
ACF_PA	12	11.03	1.64	86
ACF_SA	12	5.16	3.04	75
ACF_PH	12	10.2	NA*	NA*
ACF_SH	12	10.2	NA*	NA*

*NA-Not available

3.2. Structure and pore development of activated carbon fibre

Nitrogen adsorption is carried out to determine the effect of different chemical treatment on the pore characteristics of the produced ACF samples. Figure 1 shows the nitrogen adsorption isotherm at 77 K for the ACF sample for different acid treatment. The data for alkali treatment is unavailable due to the fact that the crystalline structure of the EFB fibre sample has been destroyed due to high concentration of alkali used. The isotherm for the acid-treated ACF samples pertain to type I isotherm of the referred IUPAC classification of physisorption isotherms [25]. Type I isotherm is indicative to the presence of micropores in the sample [17].

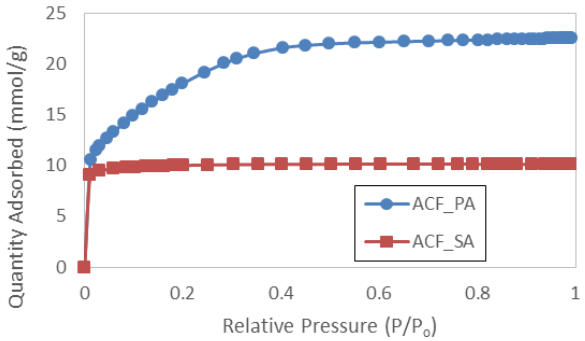

Fig. 1. Nitrogen adsorption isotherm of ACF samples.

The amount of adsorption increases over higher relative pressure (P/Po) which indicates that more pores are being formed. For the ACF_SA sample, nitrogen uptake amount increase rapidly up to a relative pressure of approximately 0.06. This large amount of nitrogen uptake at a low relative pressure is due to the enhancement of the adsorbent-adsorbate interactions in narrow micropores [25]. Due to the formation of micropores, the adsorption potential of the pore increases hence filling the pores at a low relative pressure. At high relative pressure, there would be little or no adsorption because the pores are filled with the adsorbed

adsorbate. As for the ACF_PA sample, it has shown a "knee" isotherm type I at low relative pressure. This variation of Type I isotherm where it shows that ACF_PA samples have a pore size distribution over a broad range where it includes the wider micropores and possibly narrow mesopores.

The BET surface area, total pore volume as well as the average pore diameter are presented in Table 3. Based on the data obtained, the average pore diameter of ACF_PA sample is well between the range of micropore (<2 nm) and mesopore (2 nm < pore width <50 nm). This would further prove that the ACF_PA consists of both micropores and mesopores. Whereas for the ACF_SA sample, the average pore is well within the micropore range of less than 2 nm. There is a significant difference between the 2 samples where ACF_PA has almost doubled the total pore volume and BET surface area of ACF_SA. This could be due to the excess water vaporisation via H_2SO_4 dehydration which resulted in over gasification of the sample. Thus, it reduces the BET surface area as well as the pore volume [7]. The high total pore volume is also comparable to activated carbons produced from plum kernels and kenaf biomass [14, 26].

Table 3. Pore characteristics of ACF samples.

Sample	BET Surface Area (m^2/g)	Total Pore Volume (cm^3/g)	Average Pore Diameter (nm)
ACF_PA	1493	0.782	2
ACF_SA	737	0.352	1.9

In combination with pore characterisation via nitrogen adsorption, X-ray Diffraction (XRD) was also incorporated to measure the crystalline structure of the ACF samples. The XRD patterns of the samples are shown in Fig. 2. The figure shows that 2Θ had two graphitic diffraction peaks at 23° and 44° which are assigned to the disordered 002 plane and the 10 plane [17]. Based on Fig. 2, the profiles of both ACF samples are rather similar. The peaks at 23° and 44° proves that the samples produced are made of carbon. However, there is a small peak at 72° where it corresponds to the presence of silicon in the fibre [27]. This may be possible due to the fact that the raw material of EFB fibre contains a small percentage of silica or silicon substrates [9]. The presence of silica in the ACF sample may be due to the change of silica percentage after the activation and carbonisation process. The firing of biomass may increase the silica content from 30% up to 96% [28].

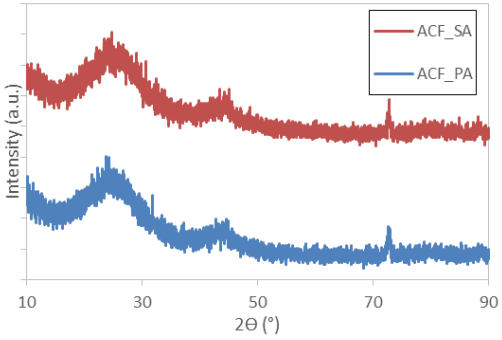

Fig. 2. X-ray diffraction patterns of ACF samples.

3.3. Surface chemistry of activated carbon fibre

Figure 3 shows the FTIR spectra of raw EFB fibre and ACF samples with different chemical treatment. The FTIR spectra of the produced ACF samples show some similarity and differences as compared to the raw EFB fibre. The peak intensity at the absorption band from 4000 cm^{-1} to 3200 cm^{-1} of raw EFB fibre is relatively higher than the ACF samples due to higher moisture content in the raw EFB fibre. Moisture removal is done during carbonisation and activation process. Thus, ACF samples have a lower peak intensity compared to the raw EFB fibre. The peak at 1748 cm^{-1} in the indicated the presence of C=O stretching of the acetyl group [29]. This acetyl group exists in the hemicellulose and lignin. The decrease of intensity of this peak in ACF samples shows the removal of cellulose, hemicellulose and lignin after chemical treatment, carbonisation and activation process. The C=C stretching vibrations of aromatic rings at 1450 cm^{-1}[30] in the ACF_SH intensified as compared to the raw EFB fibre and the intensity in ACF_SH has decreased as compared to the raw EFB fibre. The stretching of the C-O-C group is observed at 1048 cm^{-1} which is linked to the pyranoside linkage structures coming from cellulose. The presence of the P-O group at 1087 cm^{-1} represents the ionised linkage of acid phosphate esters [31].

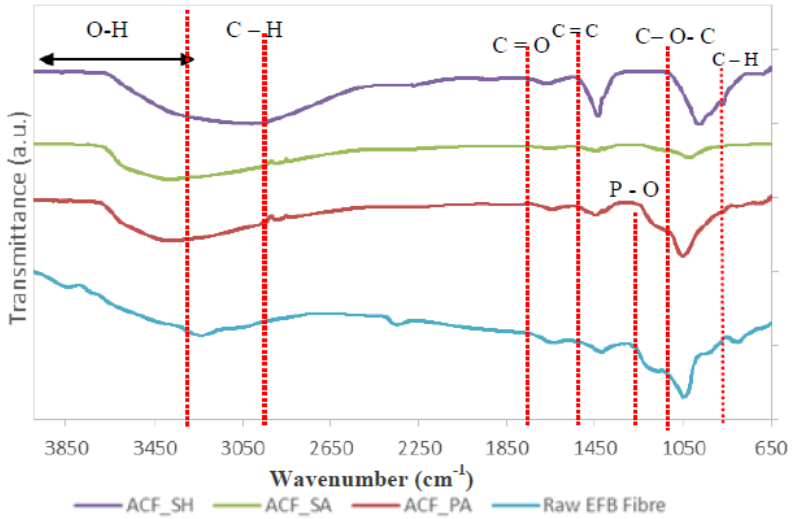

Fig. 3. FTIR spectra of ACF samples and raw EFB fibre.

3.4. Liquid phase adsorption

Urea adsorption by ACF derived from EFB fibre has already been researched on by Ooi and co-workers [7]. However, currently there is still no study done on creatinine adsorption using ACF derived from EFB fibre. Thus, the creatinine adsorption done in this work is compared to urea adsorption to evaluate the effectiveness of the ACF sample in removing both creatinine and urea. These two components are among the uremic toxins filtered out during haemodialysis.

The results of creatinine removal by the ACF samples are presented in Fig. 4. and Table 4 respectively. Creatinine removal is more effective using the ACF_PA sample as the removal of creatinine is approximately 70% compared to 54% of

the ACF_SA. This is very much comparable or even better than the conventional haemodialysis system in creatinine removal. Conventional haemodialysis membrane can remove approximately 42% of the initial creatinine level of patients [20]. Higher degrees of creatinine adsorption can be an indication towards higher surface area and presence of micro and mesopore structures [32]. Creatinine adsorption in this work shows that both ACF samples need the same amount of time to reach equilibrium which is around 20 minutes shown in Fig. 4. and Table 4. The equilibrium constant for ACF_PA and ACF_SA are 0.696 and 0.535 respectively. The higher equilibrium constant for ACF_PA indicates that the treatment using H_3PO_4 has affected and improved creatinine adsorption. Creatinine adsorption can also be governed by the BET surface area as well as the surface chemistry of the ACF sample. The higher BET surface area allows ACF_PA to adsorb more of creatinine molecules.

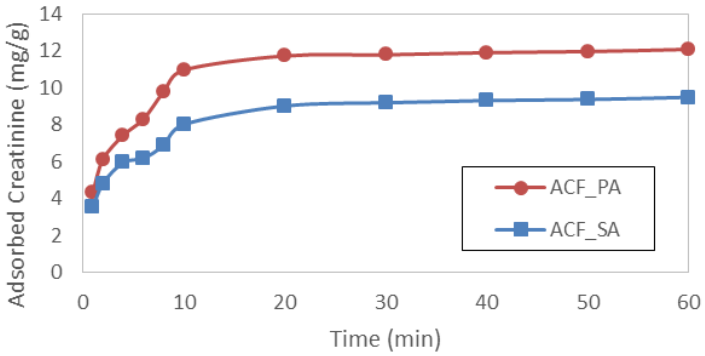

Fig. 4. Creatinine adsorption by ACF samples.

Table 4. Equilibrium time, amount of creatinine adsorbed during equilibrium and equilibrium constant for ACF samples.

Sample	Time to achieve equilibrium, t (min)	Initial Creatinine concentration, Q_o (µmol/g)	Adsorbed Creatinine concentration when equilibrium first reached, Q_{eq} (µmol/g)	Equilibrium constant , K (Q_{eq}/Q_o)
ACF_PA	20	149.01	103.69	0.696
ACF_SA	20	149.01	79.73	0.535

The results of urea adsorption by samples ACF_PA and ACF_SA are presented in Fig. 5. and Table 5. In comparison with urea adsorption, creatinine adsorption has a longer time to reach equilibrium. The smaller molecular size of urea with 60 Daltons compared with 113 Daltons of creatinine causes it to move faster [20]. Thus, the time to achieve equilibrium of 10 minutes is shorter compared to creatinine with a time of 20 minutes. The trend in urea adsorption is similar to of creatinine adsorption where sample ACF_PA is able to adsorb more urea molecules compared to sample ACF_SA with an equilibrium constant of 0.68 compared to 0.23 of sample ACF_SA. Thus, the sample ACF_PA is better in

adsorbing both urea and creatinine molecules. In comparison with conventional haemodialysis membranes, the ACF_PA sample is able to remove up to 68% of urea compared to the conventional membrane removal rate of approximately 34% in average [20]. However, ACF_SA samples has proven that treatment of EFB fibre treated with H_2SO_4 could not be compared to the conventional haemodialysis membrane as the removal rate of 23.4% is lower than the conventional haemodialysis membranes.

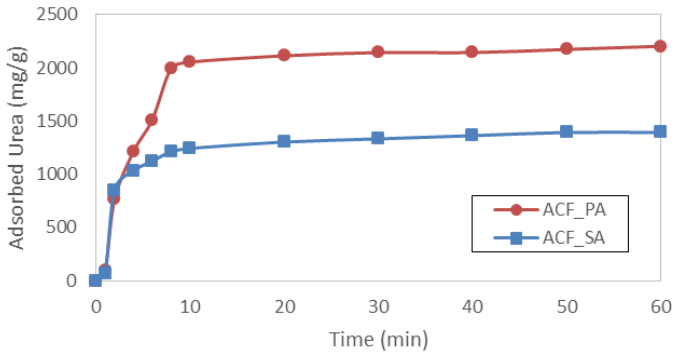

Fig. 5. Urea adsorption by ACF samples.

Table 5. Equilibrium time, amount of urea adsorbed during equilibrium and equilibrium constant for ACF samples.

Sample	Time to achieve equilibrium, t (min)	Initial Urea concentration (µmol/g)	Adsorbed urea concentration when equilibrium first reached, Q_{eq} (µmol/g)	Equilibrium constant , K (Q_{eq}/Q_o)
ACF_PA	10	50000.00	34200.05	0.684
ACF_SA	10	50000.00	11700.00	0.234

4. Conclusion

ACF samples were successfully produced by acid impregnation using H_2SO_4 (ACF_SA) and H_3PO_4 (ACF_PA). ACF samples using KOH (ACF_PH) and NaOH (ACF_SH) impregnation was not successful due to high concentrations of alkali destroying the crystalline structure of EFB fibre. This study highlights that ACF_PA proved to be better at creatinine and urea adsorption compared to ACF_SA despite having a high carbon burn-off. Combination of micro and mesopores proved to be a better option in creatinine adsorption. Both successful ACF samples perform better than conventional haemodialysis membranes in terms of creatinine and urea adsorption proving that ACF produced from EFB fibre can be used as a potential replacement for the haemodialysis membrane. Activated carbon fibre produced using H_3PO_4 showed that it has potential in future haemodialysis adsorption applications. The data produced in this study would be very beneficial for the future development of a replacement of the conventional haemodialysis membrane.

References

1. Wernert, V.; Schäf, O.; Ghobarkar, H.; and Denoyel, R. (2005). Adsorption properties of zeolites for artificial kidney applications. *Microporous and Mesoporous Materials*, 83(1), 101-113.
2. Hmwe, N.T.T.; Subramanian, P.; Tan, L.P.; and Chong, W.K. (2015). The effects of acupressure on depression, anxiety and stress in patients with hemodialysis: a randomized controlled trial. *International journal of nursing studies.* 52(2), 509-518.
3. Hakim, N.S. (2009). *Artificial Organs.* Springer-Verlag, Berlin Heidelberg.
4. Gura, V.; Davenport, A.; Beizai, M.; Ezon, C.; and Ronco, C. (2009). Beta2-microglobulin and phosphate clearances using a wearable artificial kidney: a pilot study. *American journal of kidney diseases : the official journal of the National Kidney Foundation*, 54(1), 104-111.
5. Chingombe, P.; Saha, B.; and Wakeman, R.J. (2005). Surface modification and characterisation of a coal-based activated carbon. *Carbon*, 43(15), 3132-3143.
6. Goyal, R.C.B.; and M. (2005). *Activated Carbon Adsorption*. CRC Press, United States.
7. Ooi, C.; Ang, C.; and Yeoh, F. (2013). The Properties of Activated Carbon Fiber derived from Direct Activation from Oil Palm Empty Fruit Bunch Fiber. *Advanced Material Research*, 686, 109-117.
8. Bhatnagar, A.; and Sillanpää, M. (2010). Utilization of agro-industrial and municipal waste materials as potential adsorbents for water treatment—A review. *Chemical Engineering Journal*, 157(2-3), 277-296
9. Lee, T.; Ahmad, Z.; Jamil, F.; Matsumoto, A.; and Yeoh, F., (2014). Combustion and pyrolysis of activated carbon fibre from oil palm empty fruit bunch fibre assisted through chemical activation with acid treatment. *Journal of Analytical and Applied Pyrolysis*, 110, 408-418.
10. Parshetti, G.K.; Kent Hoekman, S.; and Balasubramanian, R. (2013). Chemical, structural and combustion characteristics of carbonaceous products obtained by hydrothermal carbonization of palm empty fruit bunches. *Bioresource technology*, 135, 683-689.
11. Ioannidou, O.; and Zabaniotou, A. (2007). Agricultural residues as precursors for activated carbon production - A review. *Renewable and Sustainable Energy Reviews*, 11(9), 1966-2005.
12. Suhas; Carrott, P.J.; and Ribeiro Carrott, M.M. (2007). Lignin--from natural adsorbent to activated carbon: a review. *Bioresource technology*, 98(12), 2301-2312.
13. Viswanathan, B.; Neel, P.; and Varadarajan, T. (2009). Methods of activation and specific applications of carbon materials. *Journal for Catalysis Research*, Indian Institute of Technology Madras, 1-160.
14. Tseng, R.-L. (2007). Physical and chemical properties and adsorption type of activated carbon prepared from plum kernels by NaOH activation. *Journal of hazardous materials*, 147(3), 1020-1027.
15. Lim, W.C.; Srinivasakannan, C.; and Balasubramanian, N. (2010). Activation of palm shells by phosphoric acid impregnation for high yielding activated carbon. *Journal of Analytical and Applied Pyrolysis*, 88(2), 181-186.

16. ASTM International (2014). *ASTM D2867-09(2014)*. Standard Test Methods for Moisture in Activated Carbon.
17. Liu, W.; and Zhang, G. (2012). Effect of temperature and time on microstructure and surface functional groups of activated carbon fibers prepared from liquefied wood. *BioResources*, 7(4), 5552-5567.
18. Bellomo, R.; Kellum, J.A.; and Ronco, C. (2012). Acute kidney injury. *Lancet*, 380(9843), 756-766.
19. Upstone, S. (2000). Ultraviolet/visible light absorption spectrophotometry in clinical chemistry. *Encyclopedia of Analytical Chemistry*. Chichester: John Wiley & Sons Ltd.
20. Amin, N.; Mahmood, R.T.; Asad, M.J.; Zafar, M.; and Raja, A.M. (2014). Evaluating urea and creatinine levels in chronic renal failure pre and post dialysis : a prospective study. *Journal of Cardiovascular Disease*, 2(2), 2-5.
21. Aznar, J.S. (2011). *Characterization of activated carbon produced from coffee residues by chemical and physical activation.* Master Thesis. Chemical Engineering, KTH Chemical Science and Engineering, Sweden.
22. Mopoung, S.; Amornsakchai,P.; and Somroop, S. (2013). Characterization of phosphoric acid modified activated carbon fiber from fiber waste of pineapple leaf fiber prudction processing. *Carbon - Science and Technology*, 8(1), 314-320.
23. Kim, D.Y.; Nishiyama, Y.; Wada, M.; and Kuga, S. (2001). High-yield carbonization of cellulose by sulfuric acid impregnation. *Cellulose*, 8(1), 29-33.
24. Chen, H.Z. (2014). *Biological fundamentals for the biotechnology of lignocellulose*. In: Biotechnology of Lignocellulose. Chemical Industry Press, Beijing.
25. Thommes, M.; Kaneko, K.; Neimark, A. V.; Olivier, J.P.; Rodriguez-Reinoso, F.; Rouquerol, J.; and Sing, K.S.W. (2015). Physisorption of gases, with special reference to the evaluation of surface area and pore size distribution (IUPAC Technical Report). *Pure and Applied Chemistry*, 87(9), 1051-1069.
26. Meryemoglu, B.; Irmak, S.; and Hasanoglu, A. (2016). Production of activated carbon materials from kenaf biomass to be used as catalyst support in aqueous-phase reforming process. *Fuel Processing Technology*, 151, 59-63.
27. Chaudhari, G.N. (2011). Structural and Electrical Characterization of GaN Thin Films on Si(100). *American Journal of Analytical Chemistry*, 2, 984-988.
28. Lee, T.; Othman, R.; and Yeoh, F.Y. (2013). Development of photoluminescent glass derived from rice husk. *Biomass and Bioenergy*, 59, 380-392.
29. Weng, C.-H.; Lin, Y.-T.; and Tzeng, T.-W. (2009). Removal of methylene blue from aqueous solution by adsorption onto pineapple leaf powder. *Journal of hazardous materials*, 170(1), 417-424.
30. Stuart, B.H. (2004). *Infrared Spectroscopy: Fundamentals and Applications*, John Wiley & Sons, United States.

31. Sim, C.; Majid, S.R.; and Mahmood, N.Z. (2015). Electrochemical performance of activated carbon derived from treated food-waste. *International Journal of Electrochemical Science*, 10, 10157-10172.
32. Gergova, K.; Petrov, N.; and Minkova, V. (2007). A comparison of adsorption characteristics of various activated carbons. *Journal of Chemical Technology and Biotechnology*, 56(1), 77-82.